biomolecules

Article

Insights into the Function of a Conserved Cys120 in Human Neuroglobin in Oxidative Stress Regulation of Breast Cancer Cells

Shu-Qin Gao [1], Wen Shi [2], Si-Qi Xia [3], Zi-Lei He [3] and Ying-Wu Lin [1,3,*]

[1] Hengyang Medical College, University of South China, Hengyang 421001, China; shuqin_gao@usc.edu.cn
[2] Department of Laboratory Medicine, Yijishan Hospital of Wannan Medical College, Wuhu 241001, China; wenshi@stu.wnmc.edu.cn
[3] School of Chemistry and Chemical Engineering, University of South China, Hengyang 421001, China; siqi@stu.usc.edu.cn (S.-Q.X.); zilei.he@stu.usc.edu.cn (Z.-L.H.)
* Correspondence: ywlin@usc.edu.cn; Tel.: +86-734-8282375

Abstract

Human neuroglobin (Ngb) is a globin featuring a disulfide bond (Cys46–Cys55) and a redox-active cysteine residue (Cys120) and plays a dual role in cellular stress responses. In this study, we investigated how wild-type (WT) Ngb and its two mutants, C120S Ngb, in which Cys120 is replaced by serine, and A15C Ngb, which contains an engineered Cys15–Cys120 disulfide bridge, modulate oxidative stress in triple-negative breast cancer (MDAMB231) and hormone receptor-positive breast cancer (MCF-7) cells. In both cell lines, WT Ngb enhanced cell survival under H_2O_2-induced oxidative stress by scavenging reactive oxygen species (ROS) through oxidation of Cys120. In contrast, the C120S and A15C mutants lost this protective capacity and instead promoted apoptosis. Mass spectrometry analysis confirmed the oxidation of Cys120 to sulfenic acid in WT Ngb, whereas both mutants exhibited impaired redox activity, leading to elevated ROS levels, lipid peroxidation, and activation of caspase-9/3. AO/EB staining further revealed that WT Ngb attenuated DNA damage, while the mutants exacerbated apoptosis in both MDAMB231 and MCF-7 cells. These results demonstrate that Cys120 acts as a critical redox switch, dictating whether Ngb exerts cytoprotective or pro-apoptotic effects across different breast cancer cell types. Our findings suggest that WT Ngb may help protect normal tissues during cancer therapy, whereas engineered Ngb mutants could be used to selectively sensitize both triple-negative and hormone receptor-positive breast cancer cells to oxidative damage, offering a novel redox-targeted therapeutic strategy.

Keywords: neuroglobin; oxidative stress; redox regulation; apoptosis; breast cancer cells

Check for updates

Academic Editors: Maria Wrobel, Halina Jurkowska and Piero Crespo

Received: 24 October 2025
Revised: 29 December 2025
Accepted: 29 January 2026
Published: 31 January 2026

Copyright: © 2026 by the authors. Licensee MDPI, Basel, Switzerland. This article is an open access article distributed under the terms and conditions of the Creative Commons Attribution (CC BY) license.

1. Introduction

Breast cancer is the most commonly diagnosed cancer among women and the second leading cause of cancer-related deaths worldwide [1]. Among its subtypes, triple-negative breast cancer (TNBC) is the most aggressive and has a particularly poor prognosis, in contrast to the more treatable hormone receptor-positive types, such as those represented by the MCF-7 cell line [2,3]. Current treatments often demonstrate limited efficacy against aggressive forms like TNBC, particularly in patients with advanced or metastatic disease [2,4]. Therefore, it is important to develop new targeted drugs and immunotherapies, optimize combination treatment strategies and overcome drug resistance [4]. The inclusion of

representative models such as the TNBC cell line MDAMB231 and the hormone receptor-positive line MCF-7 in preclinical studies is crucial for a comprehensive understanding of therapeutic responses across different breast cancer subtypes.

Neuroglobin (Ngb) is a globin that was first discovered in the brains of humans and mice in 2000 [5]. It exhibits a typical 3/3 globin fold structure, with its heme iron coordinated by both proximal (His96) and distal (His64) histidine residues [6]. Functionally, Ngb plays a dual regulatory role in cellular homeostasis [7–16]. Under hypoxic/ischemic and oxidative stress conditions, Ngb exerts cytoprotective effects by suppressing cytochrome *c* (Cyt *c*)-mediated apoptotic cascades [15,17–19] and activating pro-survival signaling pathways, including G protein-PI3K/Akt [11,20,21]. Its expression levels positively correlate with post-ischemic recovery [13,18]. However, under similar stress conditions (e.g., hypoxia, reactive oxygen species, ROS) [11,16,22] or specific pathway activation (e.g., estrogen receptor signaling) [16,23], Ngb can promote tumor cell survival by modulating apoptotic and metabolic pathways. In 2021, Ngb expression was identified in estrogen receptor α-positive (ERα+) breast ductal carcinoma tissues, with higher expression levels observed in high-grade tumors than in low-grade tumors [23]. Unlike other globins, such as myoglobin and cytoglobin, Ngb was found to play a unique pro-survival role specifically in ERα+ breast cancer, correlating with tumor grade and therapeutic prognosis [11,14].

Structurally, human Ngb contains three cysteine residues at positions 46, 55, and 120. The crystal structure of human Ngb (Figure 1A) [6] showed that Cys46 and Cys55 form an intramolecular disulfide bond (Cys46–Cys55), which may control the protein stability and the binding of ligands such as O_2, CO, NO, and NO_2^- [8,24–31]. The Cys46–Cys55 disulfide bond not only indirectly modulates the redox properties of Ngb by regulating solvent reorganization and conformational changes [32], but also acts as a molecular regulator to control electron transfer to Cyt *c* under oxidative stress, thereby enabling neuroprotection to adapt to cellular redox changes [33]. The third cysteine residue, Cys120, is solvent-exposed and serves as a critical site for oxidative modifications and dimerization under stress conditions. For instance, Cys120 exhibits significant reactivity towards reactive quinones, readily forming covalent modifications that affect protein stability and function [34]. Due to its reactive nature, most biochemical and biophysical studies have employed the C120S Ngb mutant to avoid complications arising from Cys120-mediated reactions [35,36].

In a previous study, we developed an approach to protect Cys120 in human Ngb by constructing an intramolecular disulfide bond (Cys15–Cys120), as confirmed by the X-ray crystal structure of the A15C Ngb mutant (Figure 1B) [37]. This mutant exhibited significantly enhanced chemical and pH stability, as well as high thermal stability (>100 °C), compared to wild-type (WT) Ngb [38]. These properties make the A15C Ngb mutant an ideal protein scaffold for designing functional heme enzymes with peroxidase and carbene transferase activities [39–41].

In light of the documented expression of Ngb in ERα+ breast cancer and its potential role as a biomarker or therapeutic target, this study aimed to investigate its physiological function in TNBC cells, with a particular focus on its behavior under oxidative stress conditions. We performed a comparative analysis with ERα+ breast cancer cells to delineate subtype-specific responses. In addition to A15C Ngb, we engineered C120S Ngb through site-directed mutagenesis to functionally characterize the conserved Cys120 residue in human Ngb, which remains poorly understood in the context of breast cancer pathogenesis. We constructed eukaryotic expression plasmids encoding WT Ngb, C120S Ngb, and A15C Ngb, and transfected them into triple-negative breast cancer cells (MDAMB231 cells) and hormone receptor-positive breast cancer cells (MCF-7 cells), respectively. We systematically compared the ability of these Ngb variants to modulate cellular responses. Intriguingly, while WT Ngb promoted the survival of breast cancer cells under oxidative stress, the two

mutants (C120S Ngb and A15C Ngb) induced apoptosis instead. These results indicate that Cys120 acts as a critical redox-active site in the oxidative stress response of Ngb. These findings provide novel insights for the development of therapeutic strategies against breast cancers.

2. Materials and Methods

2.1. Cell Culture

The human breast cancer cell lines MDAMB231 and MCF-7 were obtained from the National Collection of Authenticated Cell Cultures (Shanghai, China). Cells were cultured in Dulbecco's Modified Eagle Medium (DMEM; Gibco, Waltham, MA, USA) supplemented with 10% fetal bovine serum (FBS, Gibco, Waltham, MA, USA) and maintained at 37 °C in a humidified 5% CO_2 atmosphere using a CO_2 incubator (Model BB150, Thermo Scientific, Waltham, MA, USA). Medium was refreshed every 48 h, and cells were passaged twice weekly upon reaching 80–90% confluency.

2.2. Generation of MDAMB231 and MCF-7 Cell Lines Overexpressing Ngb

The human WT Ngb gene and its mutants (C120S and A15C) were cloned into the pCMV-3Flag-3a eukaryotic expression vector (containing a CMV promoter, 3 × Flag tag, and neomycin resistance gene). Vector construction and sequence verification were performed by Genscript Biotech Co., Ltd (Nanjing, Jiangsu, China). MDAMB231 and MCF-7 cells were transfected with the constructs using Lipofectamine™ 3000 (Invitrogen, Waltham, MA, USA) according to the manufacturer's protocol. At 24 h post-transfection, the medium was replaced with complete growth medium supplemented with 1000 μg/mL Geneticin (G418, Macklin, Shanghai, China). The selection medium was refreshed every 2–3 days. Stable transfectants were selected under continuous G418 pressure for 4 weeks, yielding stable Ngb overexpressing cell lines.

2.3. Cell Viability Assay

Cell viability was evaluated using the MTT assay [3-(4,5-dimethylthiazol-2-yl)-2,5-diphenyltetrazolium bromide]. Stably transfected MDAMB231 cells overexpressing WT Ngb or its mutants (C120S and A15C) were assessed. MDAMB231 and MCF-7 cells were seeded in 96-well plates at 5×10^3 cells/well, allowed to adhere for 24 h, and grown to 70–80% confluency. Following treatment protocols, cells were incubated with MTT solution (0.5 mg/mL in serum-free DMEM) for 4 h at 37 °C under 5% CO_2 to facilitate formazan crystal formation. Formazan crystals were solubilized with dimethyl sulfoxide (DMSO, Damas-Beta, Shanghai, China), and absorbance was quantified at 490 nm using a Spectra Max microplate reader (Molecular Devices, San Jose, CA, USA). For oxidative stress experiments, cells were exposed to hydrogen peroxide (H_2O_2, 0.0–5.0 mM) for 12 h prior to viability assessment. Subsequent procedures were identical to the standard MTT protocol.

2.4. Detection of ROS

The detection of reactive oxygen species (ROS) was performed using a DCFH-DA ROS Assay Kit (Beyotime Biotechnology, Shanghai, China). MDAMB231 and MCF-7 cells were loaded with 10 μM DCFH-DA in serum-free medium for 30 min at 37 °C, followed by PBS washing. Fluorescence imaging was conducted using a Zeiss LSM 880 confocal laser-scanning microscope and an EVOS™ M5000 Imaging system (Invitrogen) with excitation/emission at 495/515 nm. Quantitative fluorescence analysis was performed using ZEN 3.4 software (Zeiss, Oberkochen, Germany). All experiments included three biological replicates.

2.5. MDA Assay of Lipid Peroxidation

Lipid peroxidation was assessed via malondialdehyde quantification using a commercial MDA assay system (Beyotime Biotechnology). A calibration curve was constructed through serial dilution of tetramethoxypropane standard spanning 0–20 μM concentrations. For experimental measurements, 100 μL cellular lysates of MDAMB231 and MCF-7 were combined with 200 μL thiobarbituric acid reagent solution and subjected to thermal denaturation (100 °C, 15 min). Following centrifugation (12,000× *g*, 10 min), 200 μL aliquots of supernatant were transferred to 96-well plates. Absorbance at 532 nm was spectrophotometrically assessed employing a SpectraMax microplate reader (Molecular Devices, San Jose, CA, USA). MDA concentrations were derived from the calibration curve.

2.6. Western Blot Analysis

Cellular lysates of MDAMB231 and MCF-7 cells, which had been treated with 1.5 mM H_2O_2 for 12 h prior to harvesting, were prepared using RIPA buffer supplemented with protease and phosphatase inhibitors. Proteins were separated by SDS-PAGE and electrotransferred to 0.45 μm PVDF membranes. After blocking with 5% non-fat milk/TBST (1 h, RT), membranes were incubated overnight at 4 °C with primary antibodies: cleaved caspase-9 (CST #20750S), cleaved caspase-3 (CST #9661S), anti-FLAG (DYKDDDDK Tag; CST #14793S), and β-actin (CST #4970S). Following TBST washes, membranes were probed with HRP-conjugated secondary antibody (CST #7074) for 1 h at RT. Protein bands were detected using enhanced chemiluminescence (ECL) on a Tanon 5200 Imaging System (Tanon, Shanghai, China). Band intensity quantification was performed using ImageJ software, with all experiments including three biological replicates and representative blots shown. Original western blots can be found in Supplementary Materials.

2.7. Dual AO/EB Fluorescent Staining

Acridine orange/ethidium bromide (AO/EB) dual staining was employed to assess DNA damage and apoptotic status. This method discriminates viable, apoptotic, and necrotic cells based on differential nuclear fluorescence. For experimentation, normal MDAMB231 and MCF-7 cells and the corresponding Ngb (WT, C120S and A15C) overexpressed cells were cultured with or without H_2O_2 (1.5 mM) at 37 °C under 5% CO_2 in a humidified incubator. After 12 h treatment, cells were incubated with AO/EB solution (100 μg/mL each) for 15 min at 37 °C. Fluorescence imaging was performed using a DeltaVision Elite High-Resolution System (GE Healthcare, Tanon, Shanghai, China).

2.8. Expression of Ngb Proteins in E. coli Cells

The human Ngb gene was cloned into the pET3a expression vector and heterologously expressed in *E. coli* BL21(DE3) host cells. Protein purification followed established protocols [24]. Site-directed mutagenesis was performed using the QuikChange system (Agilent Technologies, Santa Clara, CA, USA) to generate A15C and C120S mutants. All mutations were verified by Sanger sequencing, and mutant proteins were expressed and purified following identical procedures to WT Ngb [24].

2.9. ESI-Mass Analysis

High-resolution mass spectrometric analysis of the purified protein (WT, C120S and A15C) was performed using an ESI-Mass spectrometer (Waters Xevo G2-XS QTOF, Waters, Milford, MA, USA). Protein samples were buffer-exchanged into ultrapure water using PD-10 desalting columns (Sephadex G-25, Cytiva, Marlborough, MA, USA), adjusted to ~10 μM, and treated with 1 mM H_2O_2 (15 min or 2 h, RT) to investigate oxidative modifications. Prior to analysis, samples were acidified with 1% (*v*/*v*) formic acid and filtered through

0.22 µm membranes. Mass spectra were acquired in positive ion mode using MassLynx v4.2 (Waters), with molecular masses determined by MaxEnt1.

3. Results

3.1. Overexpression of Ngbs in MDAMB231 and MCF-7 Cells

Using pCMV-3Tag-3a plasmids encoding N-terminally Flag-tagged Ngb and its mutants (C102S and A15C), we established three isogenic MDAMB231 cell lines stably overexpressing the corresponding proteins. These cell lines are designated as OE-WT Ngb-MDAMB231, OE-C120S Ngb-MDAMB231, and OE-A15C Ngb-MDAMB231, respectively. Similarly, stable Ngb-overexpressing MCF-7 lines were also established and termed OE-WT Ngb-MCF-7, OE-C120S Ngb-MCF-7, and OE-A15C Ngb-MCF-7, respectively. Compared to the untransfected cells, Western blot analysis of the Flag-tag confirmed successful overexpression of the corresponding proteins in all three systems (Figure 1C,E). Consistent with previous studies documenting neuroglobin (Ngb) expression in estrogen receptor α-positive (ERα+) breast tumors and its correlation with tumor grade [23], we evaluated the basal expression of Ngb in MDAMB231 and MCF-7 cells (Supplementary Figure S1). Only minimal levels of Ngb were detected in both cell lines, which were considerably lower than those achieved by transient transfection. Under oxidative stress conditions, both endogenous and overexpressed Ngb contributed to the modulation of cellular physiology; however, the overexpressed Ngb played the predominant role in the effects observed in this study.

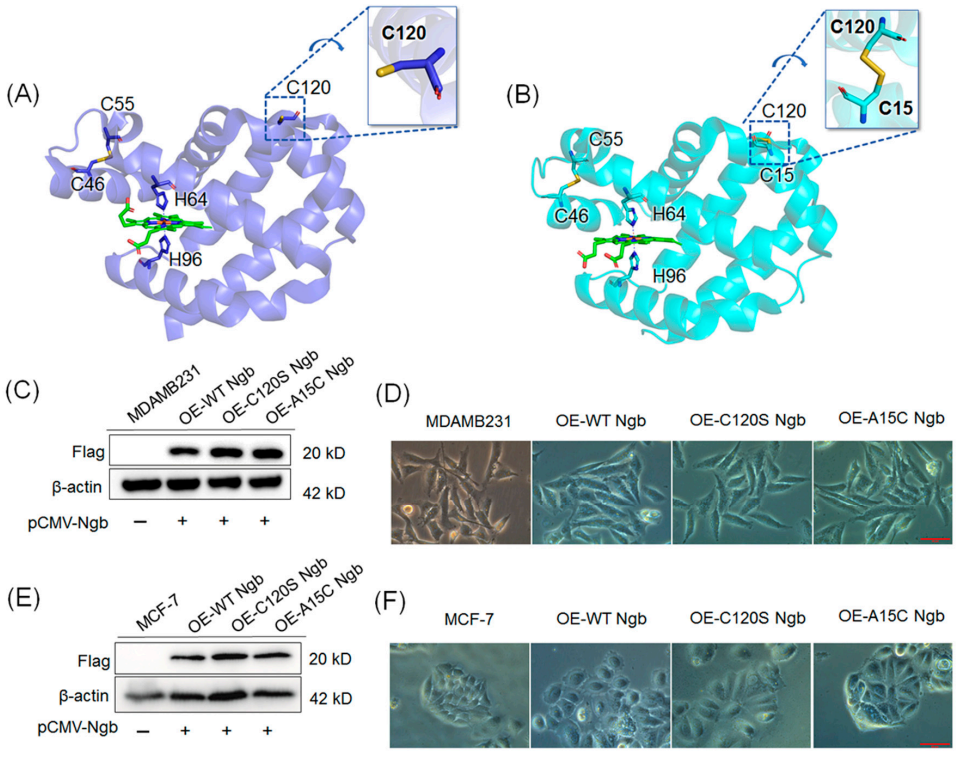


Figure 1. (**A**) Crystal structure of WT Ngb (PDB code 4MPM), showing the native Cys46–Cys55 disulfide bond, the free Cys120, and the bis-His (His64/His96) heme coordination. (**B**) Crystal structure of A15C Ngb (PDB code 7VQG), showing both the native (Cys46–Cys55) and the constructed (Cys15–Cys120) disulfide bonds. Western blot of FLAG-tagged Ngbs (WT, C120S and A15C) overexpressed in the human breast cancer cell lines MDAMB231 (**C**) and MCF-7 (**E**) using anti-FLAG antibodies. Representative phase-contrast micrographs (200× magnification) of indicated cell lines MDAMB231 (**D**) and MCF-7 (**F**), respectively. Bar = 50 µm. Original Western blot images can be found in the Supplementory Materials.

As shown in Figure 1D, certain morphological changes were observed during cell culture. The MDAMB231 cells exhibited an elongated, spindle-shaped adherent epithelial-like morphology, which is consistent with previous observations in the literature [42,43]. Overexpression of WT Ngb in MDAMB231 cells retained this spindle-shaped morphology; meanwhile, overexpression of C120S Ngb and A15C Ngb resulted in a more polygonal cell shape. As shown in Figure 1F, a similar trend was observed for MCF-7 cells, where overexpression of WT Ngb resulted in rounder cell morphology, whereas overexpression of the C120S and A15C mutants rendered the cells more polygonal. These morphological differences may be attributed to the distinct physiological regulatory roles of the three proteins within the cells.

3.2. Effects of Overexpressed Ngbs on Cell Viability

To evaluate the effects of Ngb overexpression on cell viability, we compared the proliferation of OE-WT Ngb-MDAMB231, OE-C120S Ngb-MDAMB231, and OE-A15C Ngb-MDAMB231 cells with that of the normal MDAMB231 cells. As shown in Figure 2A, no statistically significant differences in viability were observed between Ngb-overexpressing cells and normal cells under standard culture conditions (37 °C, 5% CO_2). These observations indicate that the overexpression of either WT Ngb or its mutants (C120S and A15C) has no effect on cell viability.

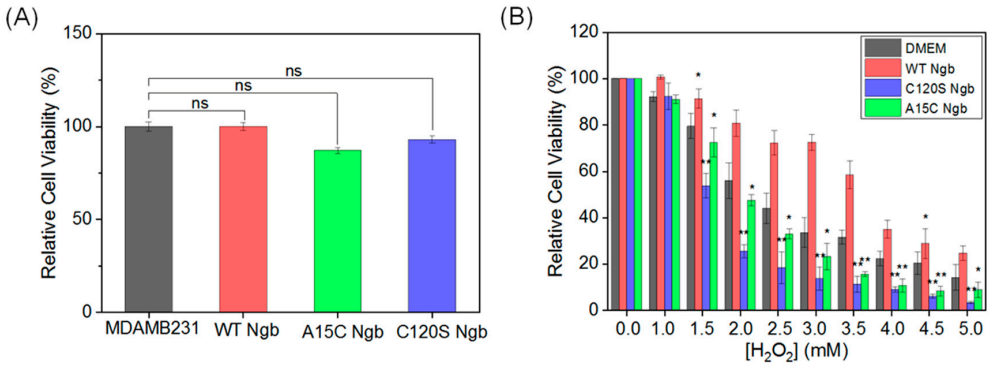


Figure 2. (**A**) Cell viability of MDAMB231 cells and Ngb (WT, A15C, or C120S) overexpressed in MDAMB231 cells. (**B**) H_2O_2 dose–response viability (0.0–5.0 mM, 12 h treatment). Data represent mean ± SEM. * $p < 0.05$, ** $p < 0.01$ vs. untreated group (DMEM). ns: not significant.

However, when the cells were co-cultured with different concentrations of H_2O_2, the three Ngb variants had different effects on viability rates. As H_2O_2 concentrations increased, OE-WT Ngb-MDAMB231 cells exhibited significantly higher viability than normal cells (DMEM group). By contrast, OE-C120S Ngb-MDAMB231 and OE-A15C Ngb-MDAMB231 cells exhibited the opposite trend, displaying markedly lower viability than normal cells and OE-WT Ngb-MDAMB231 cells. Notably, the degree of viability reduction differed between the two mutants. OE-C120S Ngb-MDAMB231 cells demonstrated the lowest survival rate, while OE-A15C Ngb-MDAMB231 cells exhibited relatively higher viability (Figure 2B). The viability results for both normal and Ngb-overexpressed MCF-7 cells showed a trend consistent with that observed for the MDAMB231 cell line, as shown in Supplementary Figure S2.

These results suggest that the state of the free Cys120 residue in each Ngb variant influences the cellular capacity to counteract oxidative stress, leading to divergent responses to H_2O_2 exposure. Based on these differential cellular responses to oxidative stress at H_2O_2 concentrations of 1.5 mM, while maintaining >55% cell viability across the experimental groups, these concentrations were systematically selected to establish well-defined oxidative stress conditions for subsequent experiments.

3.3. Effects of Overexpressed Ngbs on ROS and MDA Levels

Intracellular ROS levels were quantified using the DCFH-DA probe in normal MDAMB231 cells and the established Ngb (WT, C120S, or A15C) overexpression lines under both basal and oxidative stress conditions (Figure 3A). While no significant differences in endogenous ROS levels were observed among the cell lines under normal conditions, marked variations emerged under oxidative stress. Compared to normal cells, which showed a 75% increase in ROS, OE-WT Ngb-MDAMB231 cells demonstrated protective effects, limiting ROS elevation to ~28%. In contrast, the C120S and A15C Ngb mutants significantly exacerbated oxidative stress, with ROS levels increasing by 50% and 40%, respectively, compared to normal cell controls, and by 85% and 70%, respectively, compared to the OE-WT Ngb-MDAMB231 cells. Notably, OE-C120S Ngb-MDAMB231 cells exhibited the most severe response, with ~150% ROS elevation (Figure 3B).

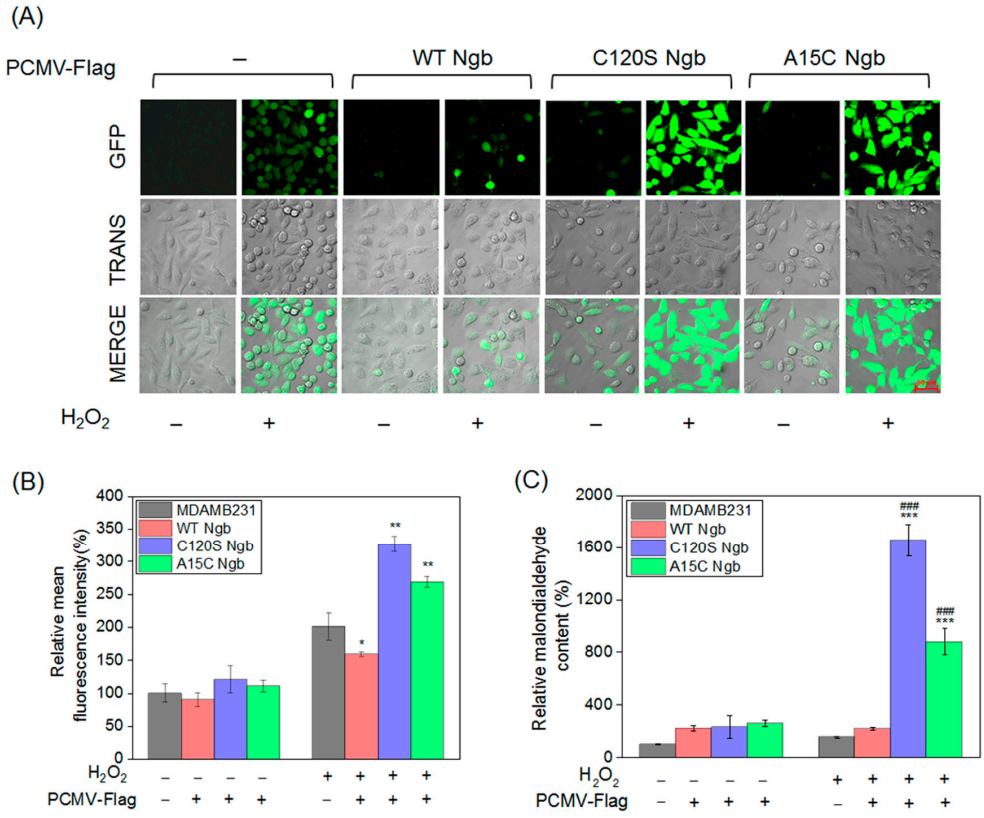


Figure 3. Comparative analysis of oxidative stress responses of MDAMB231 cells. (**A**) Confocal micrographs (200×, Zeiss LSM 880) of DCF (ROS indicator) fluorescence in MDAMB231 cells and Ngb (WT, C120S, or A15C)-overexpressed MDAMB231 cells (H_2O_2: 0.0 or 1.5 mM, 12 h). (**B**) Relative DCF fluorescence intensity. (**C**) Relative malondialdehyde levels of MDAMB231 cells and Ngb (WT, C120S, or A15C)-overexpressed MDAMB231 cells (H_2O_2: 0.0 or 1.5 mM, 12 h). Data represent mean ± SEM (n = 3). * $p < 0.05$, ** $p < 0.01$, and *** $p < 0.001$ vs. MDAMB231 cell, ### $p < 0.001$ vs. stable WT Ngb transfectant. Bar = 50 μm.

A complementary assessment of malondialdehyde (MDA) levels, which is a marker of lipid peroxidation, reinforced these observations (Figure 3C). Under oxidative stress, MDA content in OE-C120S Ngb-MDAMB231 cells increased dramatically by a factor of 9.7-fold and 7.6-fold increases in MDA content compared to MDAMB231 cells and OE-WT Ngb-MDAMB231 cells, respectively. Meanwhile, OE-A15C Ngb-MDAMB231 cells displayed elevations of 5.7-fold and 4.0-fold. These results confirm that, whereas WT Ngb mitigates oxidative damage, its C120S and A15C variants substantially amplify cellular oxidative stress responses. In line with the findings in MDAMB231 cells, the overall response of ROS

and MDA levels to Ngb overexpression was consistent in MCF-7 cells (Supplementary Figure S3).

The results showed that WT Ngb and its mutants (C120S and A15C) differentially regulate oxidative stress in breast cancer cells. WT Ngb reduces oxidative damage, whereas both mutants enhance it. This functional divergence could be attributed to the state of free Cys120 in WT Ngb. It was replaced by Ser120 in C120S Ngb and was protected by Cys15 via the disulfide bonding of Cys15–Cys120. This observation revealed a cysteine-mediated redox switch with therapeutic potential for redox-based cancer therapy.

3.4. Effects of Overexpressed Ngbs on Apoptosis Pathway

Previous studies have established that ROS can trigger mitochondrial dysfunction [14,18,19], leading to Cyt *c* release and subsequent activation of caspase-9 [11,15,19,23]. Activated caspase-9 then cleaves and activates caspase-3, initiating the apoptotic cascade [9,12,13]. To investigate the effects of Ngb overexpression on this caspase-9/3-dependent apoptotic pathway, we performed Western blot analysis to compare the levels of protein expression in normal MDAMB231 cells versus OE-WT Ngb-MDAMB231, OE-C120S Ngb-MDAMB231, and OE-A15C Ngb-MDAMB231 cells under oxidative stress conditions.

As shown in Figure 4, compared to MDAMB231 cells, OE-WT Ngb-MDAMB231 cells exhibited reduced levels of cleaved caspase-9, while both OE-C120S Ngb-MDAMB231 and OE-A15C Ngb-MDAMB231 cells showed significantly increased levels. The most pronounced elevation was observed in OE-C120S Ngb-MDAMB231 cells. The activation pattern of cleaved-caspase-3 was similar to that of cleaved-caspase-9 across all four cell types. These results demonstrate that the C120S and A15C Ngb mutants promote apoptosis under oxidative stress, whereas WT Ngb provides partial cytoprotection in MDAMB231 cells. It should be noted that, although the release of Cyt *c* from mitochondria promotes the initiation of apoptosis, our measurements reflected total cellular Cyt *c* content rather than specifically assessing the mitochondrial fraction. This may account for the absence of significant changes in expression levels observed in this study.

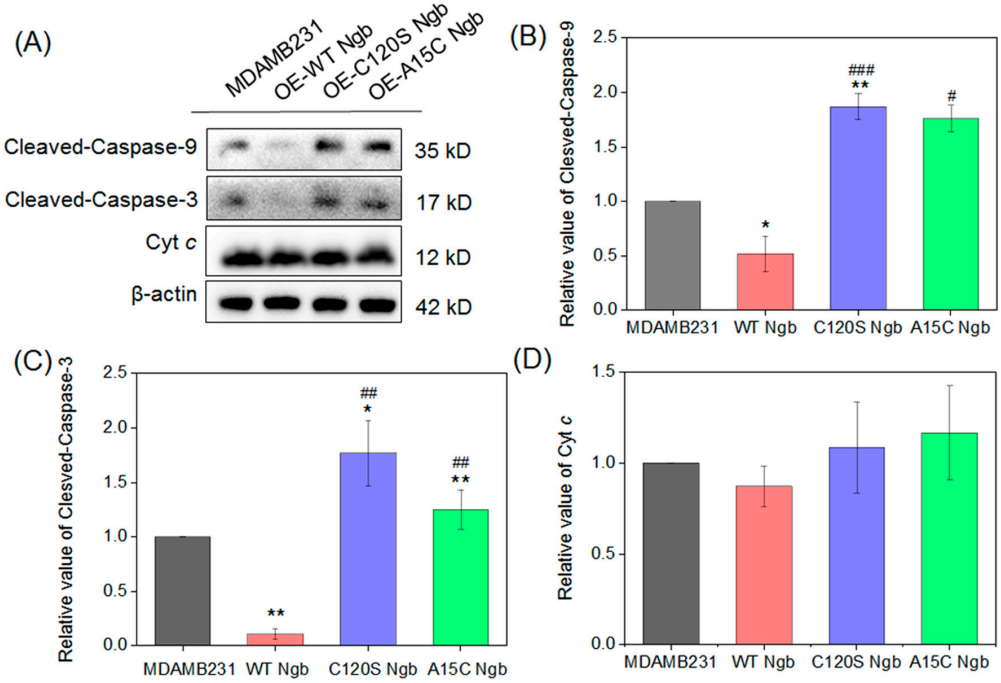


Figure 4. Apoptotic signaling in MDAMB231 cells and Ngb (WT, A15C, or C120S) overexpressed MDAMB231 cells after treatment with 1.5 mM H_2O_2 for 12 h. (**A**) Western blot of cleaved-caspase-9,

cleaved-caspase-3, Cyt *c*, and β-actin (loading control) of MDAMB231 cells and Ngb (WT, C120S, or A15C)-overexpressed MDAMB231 cells (H_2O_2: 1.5 mM, 12 h). (**B**–**D**) The statistical analysis results of the Western blots. * $p < 0.05$ and ** $p < 0.01$ vs. MDAMB231 cell; # $p < 0.05$, ## $p < 0.01$ and and ### $p < 0.001$ vs. WT Ngb. Original Western blot images can be found in the Supplementory Materials.

In MCF-7 cells (including both normal and Ngb-overexpressing cells), we observed an overall trend similar to that in the MDAMB231 cell line. As shown in Figure S4, a notable difference, however, lies in the relative levels of key apoptotic proteins. In MCF-7 cells, activation of the downstream effector cleaved caspase-3 [7,9,12] was more pronounced, particularly under conditions of C120S Ngb and A15C Ngb overexpression. This observation suggests that, under identical H_2O_2 treatment, the apoptotic process may progress more rapidly in MCF-7 cells.

3.5. Effects of Overexpressed Ngbs on H_2O_2-Induced DNA Damage and Cell Apoptosis

In MDAMB231 cells, AO/EB dual staining analysis revealed differential responses to oxidative stress in terms of DNA damage and apoptosis among cells overexpressing WT Ngb and its mutants (C120S, A15C). Untreated MDAMB231 cells (Figure 5A) showed almost no apoptosis with intact nuclear morphology, whereas H_2O_2-treated groups exhibited three distinct populations: viable cells with intact nuclei (green arrows), apoptotic cells with condensed/fragmented chromatin indicating DNA damage (red arrows), and necrotic cells with disintegrated nuclei (orange arrows) (Figure 5B–E). Overexpression of WT Ngb (Figure 5C) provided significant cytoprotection, maintaining nuclear integrity and reducing both apoptotic markers and indicators of DNA damage. In contrast, the C120S and A15C Ngb mutants (Figure 5D,E) markedly increased the apoptotic/necrotic populations, displaying prominent nuclear fragmentation and chromatin condensation.

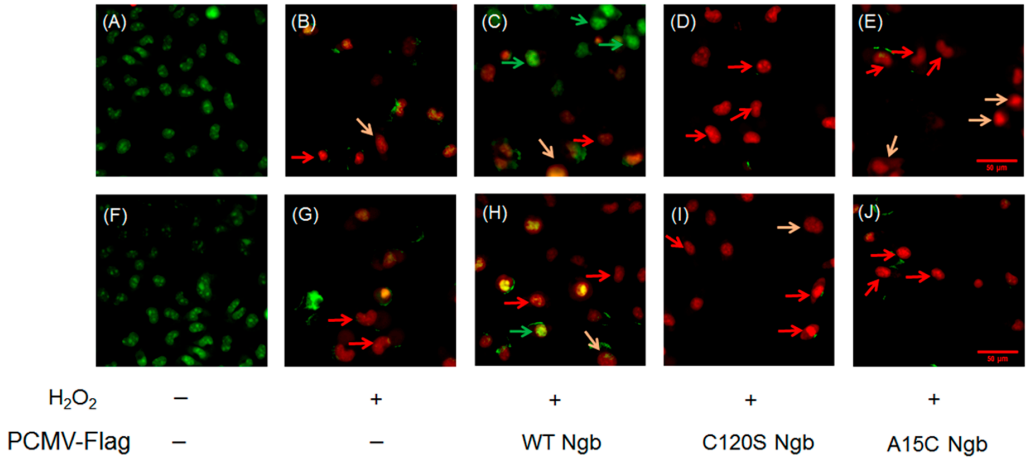


Figure 5. Apoptosis detection by AO/EB dual staining. (**A**–**E**) MDAMB231 cells and Ngb (WT, C120S, A15C) overexpressed MDAMB231 cells treated with H_2O_2 (0.0 or 1.5 mM, 12 h). (**F**–**J**) MCF-7 cells and Ngb (WT, C120S, A15C)-overexpressed MCF-7 cells treated with H_2O_2 (0.0 or 1.5 mM, 12 h). Fluorescence micrographs (400×) captured on DeltaVision High-Resolution Imaging System (GE Healthcare) excitation/emission: 488/530 nm [AO], 510/590 nm [EB]). Green arrows indicate live cells, red arrows indicate apoptotic cells, orange arrows indicate necrotic cells. Bar = 50 μm.

Similar phenomena and trends were observed for the MCF-7 cell line (Figure 5F–J). Meanwhile, compared to the OE-WT Ngb-MDAMB231 group, the OE-WT Ngb-MCF-7 group exhibited a lower proportion of viable cells, which may be related to the apoptotic pathway. This result indicates that MCF-7 cells may undergo apoptosis more rapidly under the same H_2O_2 treatment conditions.

These findings suggest that: (1) the redox-sensitive Cys120 plays a role in the regulation of WT Ngb and protects against oxidative DNA damage, (2) replacing Cys120 with Ser120 or protecting it with a disulfide bond between Cys15 and Cys120 converts Ngb into pro-apoptotic effectors that exacerbate DNA fragmentation, and (3) the Cys120-dependent redox switch in WT Ngb critically determines DNA repair capacity, chromatin stability, and the ultimate fate of the cell under oxidative stress.

3.6. ESI-Mass Analysis of Ngbs in Reaction with H_2O_2

In order to investigate the reaction of Ngb with H_2O_2, we expressed WT Ngb and its mutants (C120S and A15C Ngb) in *E. coli* cells and purified the proteins. Mass spectrometry analysis revealed three lines of evidence indicating that WT Ngb has superior H_2O_2 scavenging capacity: Firstly, the untreated samples showed a predominant peak at 16,931.0 Da (theoretical: 16,931.5 Da, Figures 6A and S5A,B), which confirmed that the WT protein had not been modified. Secondly, within 15 min of H_2O_2 exposure, the emergence of a +16 Da oxidized species was observed (experimental: 16,948.0 Da; theoretical: 16,947.5 Da, Figures 6B and S5C,D), corresponding to the oxidation of the thiol group (-SH) of Cys120 to sulfenic acid (-SOH); Thirdly, a prolonged reaction (2 h) demonstrated progressive oxidation, with an increasing the amount of the oxidized species (16,948.0 Da) being produced (Figures 6C and S5E,F), resulting in ~30% of WT Ngb being oxidized. This quantitative conversion confirms the robust capacity of WT Ngb for H_2O_2 metabolism.

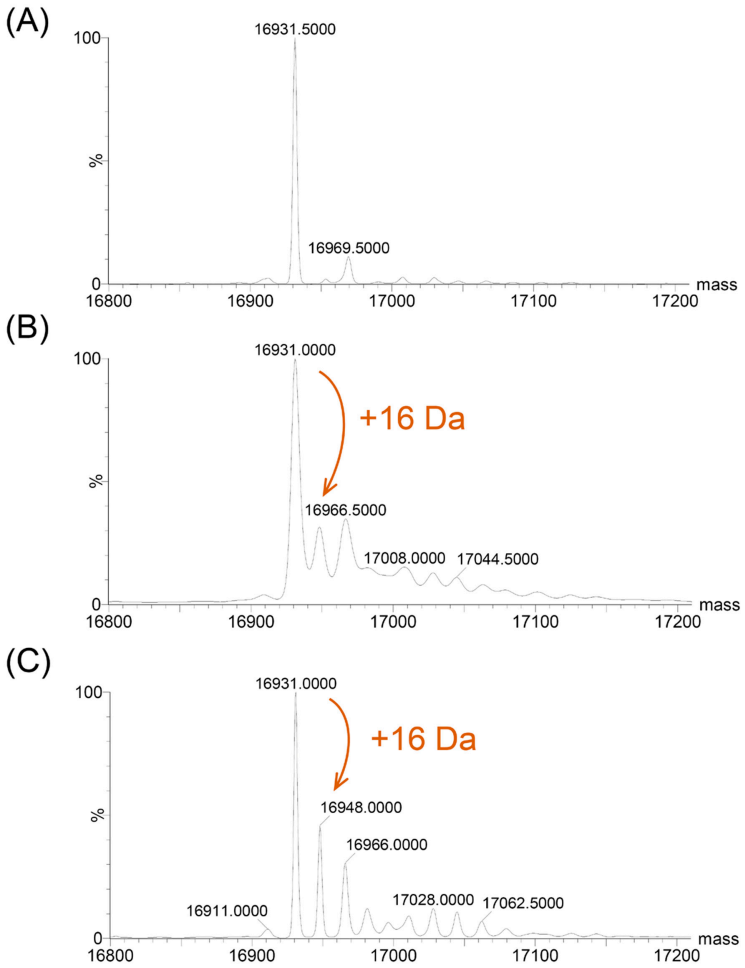


Figure 6. ESI-MS of WT Ngb oxidation by H_2O_2. (**A**) WT Ngb; (**B**) WT Ngb + 100 equiv. H_2O_2 (15 min, RT); (**C**) WT Ngb + 100 equiv. H_2O_2 (2 h, RT). Orange arrows indicate mass shifts corresponding to oxidative modifications.

Notably, neither the C120S nor the A15C mutants formed this +16 Da adduct under the same conditions (Figures S6 and S7). The C120S Ngb mutant lacks the reactive Cys120 thiol, whereas the engineered Cys15–Cys120 disulfide bond in the A15C Ngb mutant prevents the oxidation of the Cys120 thiol group. Instead, both mutants exhibited a 616 Da mass shift of the heme cofactor, indicating apo-holo transitions. Prolonged H_2O_2 exposure also caused heme dissociation. These results may explain the cellular phenotypes. The oxidation of the Cys120 thiol group in WT Ngb enables the detoxification of H_2O_2 (H_2O_2 to H_2O conversion) [7,11], thereby promoting cell survival. In contrast, the inability of the two mutants to undergo this thiol oxidation may lead to the accumulation of oxidative damage and reduced viability.

The cysteine-dependent redox switch mechanism of Ngb offers dual therapeutic potential in cancer treatment. As illustrated in Figure 7, WT Ngb could protect normal tissues during radiotherapy/chemotherapy, whereas the engineered C120S and A15C mutants of Ngb might selectively sensitize malignant cells to oxidative damage. The precise mass spectrometric characterization (with a deviation of 0.5 Da between theoretical and experimental values) validates this structure-activity relationship, providing a foundation for the development of redox-targeted therapies.

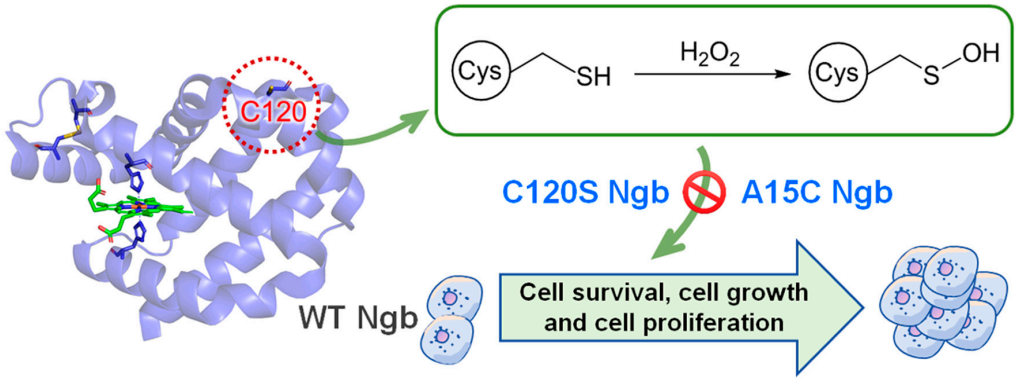


Figure 7. Proposed mechanism of Ngb-mediated H_2O_2 scavenging in breast cancer cells. Under H_2O_2-induced oxidative stress, WT Ngb protects against these effects via its catalytic Cys120 residue, which reacts with H_2O_2, resulting in oxidation of the thiol group to sulfenic acid, thereby preventing oxidative damage of the protein.

4. Discussion

Human Ngb contains a conserved Cys120 residue, the role of which remains poorly understood. The functions of WT Ngb and its mutants (C120S and A15C) were analyzed in two breast cancer cell lines (triple-negative MDAMB231 and hormone receptor-positive MCF-7). The results revealed that Cys120 may act as a critical redox switch. This switch dictates whether Ngb exerts cytoprotective or pro-apoptotic effects under oxidative stress. These findings were consistent across both breast cancer models. Under H_2O_2-induced oxidative stress, WT Ngb effectively scavenged ROS via its free Cys120 residue, significantly enhancing cell survival while mitigating lipid peroxidation, DNA damage, and activation of the caspase-9/3-mediated apoptotic pathway. This protective role was directly supported at the molecular level by mass spectrometry analysis, which confirmed that the Cys120 in WT Ngb is specifically oxidized by H_2O_2 to sulfenic acid (-SOH). The time-dependent quantitative conversion of this modification demonstrates the robust H_2O_2-metabolizing capacity of WT Ngb, providing a solid molecular basis for its cytoprotective function.

By contrast, the C120S and A15C mutants completely lost this protective capability and instead exhibited a strong pro-apoptotic phenotype. The C120S mutation directly removes the redox-active residue, whereas the engineered Cys15–Cys120 disulfide bond in the A15C

mutant effectively blocks Cys120, preventing its participation in redox reactions. Mass spectrometry confirmed that neither mutant formed the Cys120-SOH adduct. This loss of function at the molecular level directly translated to cellular outcomes: ROS accumulation, exacerbated oxidative damage, and increased sensitivity to apoptosis. Notably, the C120S mutant consistently demonstrated the most potent pro-oxidant and pro-apoptotic effects across all assays, suggesting that complete removal of Cys120 has a more profound impact on protein function than its protection via an engineered disulfide bond.

4.1. Therapeutic Implications and Translational Prospects

The Cys120-dependent redox switch mechanism revealed by this study indicates that Ngb may have dual functions in response to oxidative stress, such as that caused by radiotherapy and certain chemotherapies. On one hand, WT Ngb presents a potential strategy for protecting normal tissues. Radiotherapy and many chemotherapeutic agents exert their cytotoxic effects partly through the generation of large amounts of ROS [44,45], which is also a major cause of damage to normal tissues [46]. Based on its established role in other models, supplementing with WT Ngb may, in theory, help to mitigate the side effects experienced by tissues that are highly susceptible to oxidative damage, such as neurons [7,11,18,33,47] and cardiomyocytes [7,9]. However, his potential application requires further validation in specific normal tissue models, as the protective efficacy of WT Ngb can be context-dependent, as also observed in some of our experiments.

On the other hand, engineered Ngb mutants (C120S and A15C) could function as sensitizing agents for tumor cells. Given the lack of effective targeted therapies for aggressive cancers like triple-negative breast cancer [2–4], utilizing Ngb mutants that lack ROS-scavenging capacity could present a potential strategy by potentiating intracellular oxidative stress. These mutants could selectively sensitize cancer cells to conventional treatments or directly induce apoptosis. The observed sensitizing effects of these mutants in two distinct molecular subtypes of breast cancer indicate the potential applicability of this approach to different contexts of breast cancer.

4.2. Limitations and Future Directions

Although our study sheds light on the mechanism in cellular models, translating these findings into clinical applications requires overcoming several challenges, which also represent important directions for future research.

First, in vivo delivery efficiency presents a major translational hurdle. It is paramount to achieve the efficient and targeted delivery of Ngb and its mutants to specific tissues (e.g., tumors or normal organs requiring protection). Future work should therefore focus on exploring suitable delivery systems, such as viral vectors, exosomes, or nanoparticles, to enable the targeted expression or function of Ngb proteins in vivo.

Second, tumor heterogeneity and cell-type-specific responses could affect treatment uniformity. The intrinsic redox status varies greatly among different tumor types and even among cells within the same tumor. This heterogeneity may modulate the functional outcomes of Ngb mutants. Therefore, validating their efficacy in more complex animal models that better mimic the human tumor microenvironment (e.g., patient-derived xenograft models) is a necessary step towards clinical translation.

5. Conclusions

This study elucidates the critical role of Cys120 in human neuroglobin (Ngb) as a redox-sensitive switch that modulates cellular responses to oxidative stress in both triple-negative breast cancer (TNBC) and hormone receptor-positive (HR+) breast cancer cells. In TNBC MDAMB231 cells, WT Ngb exhibited cytoprotective effects by scavenging ROS through

Cys120-mediated H_2O_2 detoxification. This protective function was consistently observed in HR+ MCF-7 cells, where WT Ngb similarly reduced oxidative damage. However, the C120S and A15C Ngb mutants lost this protective capability in both cell types and instead promoted apoptosis under oxidative stress. Mass spectrometry analyses confirmed that WT Ngb undergoes oxidation of Cys120 to sulfenic acid (-SOH), while the mutants fail to engage in this redox mechanism, leading to exacerbated oxidative damage, lipid peroxidation, and activation of apoptotic pathways (caspase-9/3). Notably, the apoptotic response was more pronounced in MCF-7 cells, consistent with their observed higher sensitivity to H_2O_2-induced stress.

Therefore, these findings highlight the dual therapeutic potential for Ngb in cancer treatment: First, WT Ngb may be investigated further as a protective agent against the side effects of radiotherapy or chemotherapy associated with oxidative damage in normal tissues. Second, engineered Ngb mutants (C120S or A15C) may selectively sensitize cancer cells to oxidative stress, offering a new strategy for targeted redox-based therapies in aggressive cancers such as TNBC, as well as HR+ breast cancers. Although the protective role of WT Ngb in normal tissues requires further validation and its applicability to other cancers remains to be determined, this study provides an important foundation and suggests future directions for developing anti-cancer therapies based on protein redox engineering.

Supplementary Materials: The following supporting information can be downloaded at: https://www.mdpi.com/article/10.3390/biom16020215/s1, Figure S1: Western blot analysis of basal Ngb expression levels in MCF-7 and MDAMB231 cell lines, using an anti-Ngb antibody. β-Actin was used as a loading control; Figure S2: (A) Cell viability of MCF-7 cells and Ngb (WT, A15C, or C120S)-overexpressed MCF-7 cells. (B) H_2O_2 dose-response viability (0.0–5.0 mM, 12 h treatment). Data represent mean ± SEM. * $p < 0.05$, ** $p < 0.01$ vs. untreated group (DMEM); Figure S3: Comparative analysis of oxidative stress responses of MCF-7 cells. (A) Confocal micrographs (200×, Zeiss LSM 880) of DCF (ROS indicator) fluorescence in MCF-7 cells, and Ngb (WT, C120S, or A15C)-overexpressed MCF-7 cells (H_2O_2: 0.0 or 1.5 mM, 12 h). (B) Relative DCF fluorescence intensity. (C) Relative malondialdehyde levels. Data represent mean ± SEM ($n = 3$). * $p < 0.05$, ** $p < 0.01$ vs. MDAMB231 cell, # $p < 0.05$, ## $p < 0.01$ vs. stable WT Ngb transfectant. Bar = 50 μm; Figure S4: Apoptotic signaling in MCF-7 cells and Ngb (WT, A15C, or C120S)-overexpressed MCF-7 cells after treatment with 1.5 mM H_2O_2 for 12 h. (A) Western blot of cleaved-caspase-9, cleaved-caspase-3, cytochrome *c* (Cyt *c*), and β-actin (loading control) of MCF-7cell, Ngb (WT, C120S, orA15C)-overexpressed MCF-7 cells (H_2O_2: 1.5 mM, 12 h). (B–D) The statistical analysis results of the Western blots. * $p < 0.05$ and ** $p < 0.01$ vs. MDAMB231cell; # $p < 0.05$ and ## $p < 0.01$ vs. WT Ngb; Figure S5: ESI-MS analysis of WT Ngb oxidation induced by H_2O_2. (A,C,E) Original multi-charge series: (A) WT Ngb, (C) +100 equiv. H_2O_2 (15 min, RT), (E) +100 equiv. H_2O_2 (2 h, RT). (B,D,F) The MaxEnt survey spectrum showing the molecular mass shifts. (B) WT Ngb, (D) +100 equiv. H_2O_2 (15 min, RT), (F) +100 equiv. H_2O_2 (2 h, RT). Molecular weight of WT Ngb, theoretical: 16,931.5 Da, experimental: 16,931.5/16,931.0 Da. Molecular weight of oxidized WT Ngb (+16 Da), theoretical: 16,947.5 Da, experimental: 16,948.0 Da; Figure S6: ESI-MS analysis of C120S Ngb oxidation induced by H_2O_2. (A,C) Original multi-charge series: (A) C120S Ngb, (C) +100 equiv. H_2O_2 (2 h, RT). (B,D) The MaxEnt survey spectrum. (B) C120S Ngb, (D) +100 equiv. H_2O_2 (2 h, RT). Molecular weight of the apo-protein of C120S Ngb, theoretical: 16,915.5 Da; experimental: 16,915.5/16,916.5 Da. Molecular weight of the Holo-protein of C120S Ngb, theoretical: 17,531.5 Da; experimental: 17,531.0, or 17,532.0 Da; Figure S7: ESI-MS analysis of A15C Ngb oxidation induced by H_2O_2. (A,C) Original multi-charge series: (A) A15C Ngb, (C) +100 equiv. H_2O_2 (2 h, RT). (B,D) The MaxEnt survey spectrum. (B) A15C Ngb, (D) +100 equiv. H_2O_2 (2 h, RT). Molecular weight of the apo-protein of A15C Ngb, theoretical: 16,961.5 Da; experimental: 16,961.5 Da. Molecular weight of the holo-protein of A15C Ngb, theoretical: 17,576.5 Da; experimental: 17,576.5/17,577.5 Da. Original western blots.

Author Contributions: Conceptualization, Y.-W.L.; methodology, S.-Q.G., W.S., S.-Q.X. and Z.-L.H.; validation, Y.-W.L.; investigation, S.-Q.G., W.S., S.-Q.X. and Z.-L.H.; data curation, S.-Q.G., W.S., S.-Q.X. and Z.-L.H.; writing—original draft preparation, S.-Q.G., W.S., S.-Q.X. and Z.-L.H.; writing—review and editing, Y.-W.L.; supervision, Y.-W.L.; project administration, Y.-W.L.; funding acquisition, S.-Q.G. and Y.-W.L. All authors have read and agreed to the published version of the manuscript.

Funding: This project was supported by the Research Foundation of the Education Bureau of Hunan Province, China (Grant No. 23B0400) and the National Natural Science Foundation of China (Grant No. 32171270).

Institutional Review Board Statement: The study was conducted in accordance with the Declaration of Helsinki and approved by the Medical Ethics Committee of the University of South China (protocol code: 2024-105; date of approval: 6 January 2024).

Informed Consent Statement: Not applicable.

Data Availability Statement: The original contributions presented in this study are included in the article/Supplementary Material. Further inquiries can be directed to the corresponding author.

Conflicts of Interest: The authors declare no conflicts of interest.

References

1. Sung, H.; Ferlay, J.; Siegel, R.L.; Laversanne, M.; Soerjomataram, I.; Jemal, A.; Bray, F. Global Cancer Statistics 2020: GLOBOCAN Estimates of Incidence and Mortality Worldwide for 36 Cancers in 185 Countries. *CA Cancer J. Clin.* **2021**, *71*, 209–249. [CrossRef]
2. Li, Y.; Zhang, H.; Merkher, Y.; Chen, L.; Liu, N.; Leonov, S.; Chen, Y. Recent advances in therapeutic strategies for triple-negative breast cancer. *J. Hematol. Oncol.* **2022**, *15*, 121. [CrossRef]
3. Derakhshan, F.; Reis-Filho, J.S. Pathogenesis of Triple-Negative Breast Cancer. *Annu. Rev. Pathol.* **2022**, *17*, 181–204. [CrossRef]
4. Leon-Ferre, R.A.; Goetz, M.P. Advances in systemic therapies for triple negative breast cancer. *BMJ* **2023**, *381*, e071674. [CrossRef] [PubMed]
5. Burmester, T.; Weich, B.; Reinhardt, S.; Hankeln, T. A vertebrate globin expressd in the brain. *Nature* **2000**, *407*, 520–523. [CrossRef]
6. Guimaraes, B.G.; Hamdane, D.; Lechauve, C.; Marden, M.C.; Golinelli-Pimpaneau, B. The crystal structure of wild-type human brain neuroglobin reveals flexibility of the disulfide bond that regulates oxygen affinity. *Biol. Crystallogr.* **2014**, *70*, 1005–1014. [CrossRef]
7. Burmester, T.; Hankeln, T. What is the function of neuroglobin? *J. Exp. Biol.* **2009**, *212*, 1423–1428. [CrossRef] [PubMed]
8. Tiso, M.; Tejero, J.; Basu, S.; Azarov, I.; Wang, X.; Simplaceanu, V.; Frizzell, S.; Jayaraman, T.; Geary, L.; Shapiro, C.; et al. Human neuroglobin functions as a redox-regulated nitrite reductase. *J. Biol. Chem.* **2011**, *286*, 18277–18289. [CrossRef]
9. Ascenzi, P.; di Masi, A.; Leboffe, L.; Fiocchetti, M.; Nuzzo, M.T.; Brunori, M.; Marino, M. Neuroglobin: From structure to function in health and disease. *Mol. Asp. Med.* **2016**, *52*, 1–48. [CrossRef]
10. Fiocchetti, M.; Cipolletti, M.; Brandi, V.; Polticelli, F.; Ascenzi, P. Neuroglobin and friends. *J. Mol. Recognit.* **2017**, *30*, e2654. [CrossRef]
11. Fiocchetti, M.; Fernandez, V.S.; Montalesi, E.; Marino, M. Neuroglobin: A Novel Player in the Oxidative Stress Response of Cancer Cells. *Oxidative Med. Cell. Longev.* **2019**, *2019*, 6315034. [CrossRef] [PubMed]
12. Gorabi, A.M.; Aslani, S.; Barreto, G.E.; Baez-Jurado, E.; Kiaie, N.; Jamialahmadi, T.; Sahebkar, A. The potential of mitochondrial modulation by neuroglobin in treatment of neurological disorders. *Free Radic. Biol. Med.* **2021**, *162*, 471–477. [CrossRef]
13. De Simone, G.; Sbardella, D.; Oddone, F.; Pesce, A.; Coletta, M.; Ascenzi, P. Structural and (Pseudo-)Enzymatic Properties of Neuroglobin: Its Possible Role in Neuroprotection. *Cells* **2021**, *10*, 3366. [CrossRef]
14. Barreto, G.E.; McGovern, A.J.; Garcia-Segura, L.M. Role of Neuroglobin in the Neuroprotective Actions of Estradiol and Estrogenic Compounds. *Cells* **2021**, *10*, 1907. [CrossRef]
15. Fiocchetti, M.; Cracco, P.; Montalesi, E.; Solar Fernandez, V.; Stuart, J.A.; Marino, M. Neuroglobin and mitochondria: The impact on neurodegenerative diseases. *Arch. Biochem. Biophys.* **2021**, *701*, 108823. [CrossRef]
16. Marino, M.; Misasi, R.; Ruoppolo, M. Editorial for Special Issue: Neuroglobin from Brain Protection to Cancer Progression. *Cells* **2022**, *11*, 2181. [CrossRef]
17. Fordel, E.; Thijs, L.; Moens, L.; Dewilde, S. Neuroglobin and cytoglobin expression in mice. Evidence for a correlation with reactive oxygen species scavenging. *FEBS J.* **2007**, *274*, 1312–1317. [CrossRef]
18. Chan, A.S.; Saraswathy, S.; Rehak, M.; Ueki, M.; Rao, N.A. Neuroglobin protection in retinal ischemia. *Investig. Ophthalmol. Vis. Sci.* **2012**, *53*, 704–711. [CrossRef]

19. Yanez, I.M.; Torres-Cuevas, I.; Corral-Debrinski, M. Neuroglobin: A promising candidate to treat neurological diseases. *Neural Regen. Res.* **2026**, *21*, 1292–1303. [CrossRef] [PubMed]
20. Li, L.; Liu, Q.R.; Xiong, X.X.; Liu, J.M.; Lai, X.J.; Cheng, C.; Pan, F.; Chen, Y.; Yu, S.B.; Yu, A.C.; et al. Neuroglobin promotes neurite outgrowth via differential binding to PTEN and Akt. *Mol. Neurobiol.* **2014**, *49*, 149–162. [CrossRef] [PubMed]
21. Cai, B.; Li, W.; Mao, X.; Winters, A.; Ryou, M.G.; Liu, R.; Greenberg, D.A.; Wang, N.; Jin, K.; Yang, S.H. Neuroglobin Overexpression Inhibits AMPK Signaling and Promotes Cell Anabolism. *Mol. Neurobiol.* **2016**, *53*, 1254–1265. [CrossRef]
22. Hieu, V.N.; Thuy, L.T.T.; Hai, H.; Dat, N.Q.; Hoang, D.V.; Hanh, N.V.; Phuong, D.M.; Hoang, T.H.; Sawai, H.; Shiro, Y.; et al. Capacity of extracellular globins to reduce liver fibrosis via scavenging reactive oxygen species and promoting MMP-1 secretion. *Redox Biol.* **2022**, *52*, 102286. [CrossRef] [PubMed]
23. Solar Fernandez, V.; Fiocchetti, M.; Cipolletti, M.; Segatto, M.; Cercola, P.; Massari, A.; Ghinassi, S.; Cavaliere, F.; Marino, M. Neuroglobin: A New Possible Marker of Estrogen-Responsive Breast Cancer. *Cells* **2021**, *10*, 1986. [CrossRef]
24. Dewilde, S.; Kiger, L.; Burmester, T.; Hankeln, T.; Baudin-Creuza, V.; Aerts, T.; Marden, M.C.; Caubergs, R.; Moens, L. Biochemical characterization and ligand binding properties of neuroglobin, a novel member of the globin family. *J. Biol. Chem.* **2001**, *276*, 38949–38955. [CrossRef] [PubMed]
25. Hamdane, D.; Kiger, L.; Dewilde, S.; Green, B.N.; Pesce, A.; Uzan, J.; Burmester, T.; Hankeln, T.; Bolognesi, M.; Moens, L.; et al. The redox state of the cell regulates the ligand binding affinity of human neuroglobin and cytoglobin. *J. Biol. Chem.* **2003**, *278*, 51713–51721. [CrossRef] [PubMed]
26. Van Doorslaer, S.; Dewilde, S.; Kiger, L.; Nistor, S.V.; Goovaerts, E.; Marden, M.C.; Moens, L. Nitric oxide binding properties of neuroglobin. A characterization by EPR and flash photolysis. *J. Biol. Chem.* **2003**, *278*, 4919–4925. [CrossRef]
27. Astudillo, L.; Bernad, S.; Derrien, V.; Sebban, P.; Miksovska, J. Conformational dynamics in human neuroglobin: Effect of His64, Val68, and Cys120 on ligand migration. *Biochemistry* **2012**, *51*, 9984–9994. [CrossRef]
28. Trashin, S.; de Jong, M.; Luyckx, E.; Dewilde, S.; De Wael, K. Electrochemical Evidence for Neuroglobin Activity on NO at Physiological Concentrations. *J. Biol. Chem.* **2016**, *291*, 18959–18966. [CrossRef]
29. Wu, L.B.; Yuan, H.; Gao, S.Q.; You, Y.; Nie, C.M.; Wen, G.B.; Lin, Y.W.; Tan, X. Regulating the nitrite reductase activity of myoglobin by redesigning the heme active center. *Nitric Oxide Biol. Chem.* **2016**, *57*, 21–29. [CrossRef]
30. Williams, M.D.; Ragireddy, V.; Dent, M.R.; Tejero, J. Engineering neuroglobin nitrite reductase activity based on myoglobin models. *Biochem. Biophys. Rep.* **2023**, *36*, 101560. [CrossRef]
31. Caselli, M.; Sebastianelli, L.; Meglioli, M.; Battistuzzi, G.; Borsari, M. Influence of the intramolecular disulfide Cys46–Cys55 bridge on the interaction of human neuroglobin with SDS. *J. Inorg. Biochem.* **2025**, *274*, 113109. [CrossRef]
32. Bellei, M.; Bortolotti, C.A.; Di Rocco, G.; Borsari, M.; Lancellotti, L.; Ranieri, A.; Sola, M.; Battistuzzi, G. The influence of the Cys46/Cys55 disulfide bond on the redox and spectroscopic properties of human neuroglobin. *J. Inorg. Biochem.* **2018**, *178*, 70–86. [CrossRef]
33. Semenova, M.A.; Chertkova, R.V.; Kirpichnikov, M.P.; Dolgikh, D.A. Molecular Interactions between Neuroglobin and Cytochrome c: Possible Mechanisms of Antiapoptotic Defense in Neuronal Cells. *Biomolecules* **2023**, *13*, 1233. [CrossRef]
34. Nicolis, S.; Monzani, E.; Pezzella, A.; Ascenzi, P.; Sbardella, D.; Casella, L. Neuroglobin modification by reactive quinone species. *Chem. Res. Toxicol.* **2013**, *26*, 1821–1831. [CrossRef] [PubMed]
35. Bocahut, A.; Derrien, V.; Bernad, S.; Sebban, P.; Sacquin-Mora, S.; Guittet, E.; Lescop, E. Heme orientation modulates histidine dissociation and ligand binding kinetics in the hexacoordinated human neuroglobin. *J. Biol. Inorg. Chem.* **2013**, *18*, 111–122. [CrossRef] [PubMed]
36. Cassiani, A.; Furtmüller, P.G.; Borsari, M.; Battistuzzi, G.; Hofbauer, S. Insights into heme degradation and hydrogen peroxide-induced dimerization of human neuroglobin. *Biosci. Rep.* **2025**, *45*, 1–13. [CrossRef]
37. Gao, S.Q.; Yuan, H.; Liu, X.C.; Li, L.; Tan, X.; Wen, G.B.; Lin, Y.W. The X-ray crystal structure of human A15C neuroglobin reveals both native/de novo disulfide bonds and unexpected ligand-binding sites. *Proteins* **2022**, *90*, 1152–1158. [CrossRef]
38. Liu, H.X.; Li, L.; Yang, X.Z.; Wei, C.W.; Cheng, H.M.; Gao, S.Q.; Wen, G.B.; Lin, Y.W. Enhancement of protein stability by an additional disulfide bond designed in human neuroglobin. *RSC Adv.* **2019**, *9*, 4172–4179. [CrossRef] [PubMed]
39. Chen, S.F.; Liu, X.C.; Xu, J.K.; Li, L.; Lang, J.J.; Wen, G.B.; Lin, Y.W. Conversion of Human Neuroglobin into a Multifunctional Peroxidase by Rational Design. *Inorg. Chem.* **2021**, *60*, 2839–2845. [CrossRef]
40. Sun, L.J.; Wang, H.; Xu, J.K.; Gao, S.Q.; Wen, G.B.; Lin, Y.W. Exploiting and Engineering Neuroglobin for Catalyzing Carbene N-H Insertions and the Formation of Quinoxalinones. *Inorg. Chem.* **2023**, *62*, 16294–16298. [CrossRef]
41. Sun, L.J.; Wang, H.; Xu, J.K.; Niu, W.; Gao, S.Q.; Lin, Y.W. Engineering Neuroglobin for Synthesis of Chiral Organoborons via Carbene B-H Insertion. *Org. Lett.* **2024**, *26*, 8872–8877. [CrossRef]
42. Li, P.; Butcher, N.J.; Minchin, R.F. Effect arylamine N-acetyltransferase 1 on morphology, adhesion, migration, and invasion of MDA-MB-231 cells: Role of matrix metalloproteinases and integrin alphaV. *Cell Adhes. Migr.* **2020**, *14*, 1–11. [CrossRef]
43. Jost, T.A.; Gardner, A.L.; Morgan, D.; Brock, A. Deep learning identifies heterogeneous subpopulations in breast cancer cell lines. *bioRxiv* **2024**, *2024*, 1–21. [CrossRef]

44. Glorieux, C.; Liu, S.; Trachootham, D.; Huang, P. Targeting ROS in cancer: Rationale and strategies. *Nat. Rev. Drug Discov.* **2024**, *23*, 583–606. [CrossRef]
45. Lei, G.; Zhang, Y.; Koppula, P.; Liu, X.; Zhang, J.; Lin, S.H.; Ajani, J.A.; Xiao, Q.; Liao, Z.; Wang, H.; et al. The role of ferroptosis in ionizing radiation-induced cell death and tumor suppression. *Cell Res.* **2020**, *30*, 146–162. [CrossRef] [PubMed]
46. Finkel, T.; Holbrook, N.J. Oxidants, oxidative stress and the biology of ageing. *Nature* **2000**, *408*, 239–247. [CrossRef]
47. Wang, X.; Liu, J.; Zhu, H.; Tejima, E.; Tsuji, K.; Murata, Y.; Atochin, D.N.; Huang, P.L.; Zhang, C.; Lo, E.H. Effects of Neuroglobin Overexpression on Acute Brain Injury and Long-Term Outcomes After Focal Cerebral Ischemia. *Stroke* **2008**, *39*, 1869–1874. [CrossRef] [PubMed]

Disclaimer/Publisher's Note: The statements, opinions and data contained in all publications are solely those of the individual author(s) and contributor(s) and not of MDPI and/or the editor(s). MDPI and/or the editor(s) disclaim responsibility for any injury to people or property resulting from any ideas, methods, instructions or products referred to in the content.